

# Animal Model

## Microglial Response to Amyloid Plaques in APPsw Transgenic Mice

Sally A. Frautschy, Fusheng Yang,  
Michael Irrizarry, Brad Hyman, T. C. Saido,  
Karen Hsiao, and Greg M. Cole

From the Sepulveda Veterans Affairs Medical Center, GRECC,  
and Departments of Medicine and Neurology, University of  
California, Los Angeles, Sepulveda, California

**Microglial activation is central to the inflammatory response in Alzheimer's Disease (AD). A recently described mouse line, Tg(HuAPP695.K670N/M671L)2576, expressing human amyloid precursor protein with a familial AD gene mutation, age-related amyloid deposits, and memory deficits, was found to develop a significant microglial response using *Griffonia simplicifolia* lectin or phosphotyrosine probe to identify microglia. Both *Griffonia simplicifolia* lectin and phosphotyrosine staining showed increased numbers of intensely labeled, often enlarged microglia clustered in and around plaques, consistent with microglial activation related to  $\beta$ -amyloid formation. Using quantitative image analysis of coronal phosphotyrosine-immunostained sections, transgene-positive 10- to 16-month-old, hemizygous, hybrid Tg2576 (APPsw) animals showed significantly increased microglial density and size in plaque-forming areas of hippocampus and frontal, entorhinal, and occipital cortex. Quantitative analysis of microglia as a function of distance from the center of plaques (double labeled for  $A\beta$  peptide and microglia) revealed highly significant, two- to fivefold elevations in microglial number and area within plaques compared with neighboring regions. Tg2576  $\beta$ -amyloid-plaque-forming mice should be a useful system for assessing the consequences of the microglial-mediated inflammatory response to  $\beta$ -amyloid and developing anti-inflammatory therapeutic strategies for Alzheimer's disease. These results provide the first quantitative link between  $\beta$ -amyloid plaque formation and microglial activation in an animal model with neuritic plaques and memory deficits. (*Am J Pathol* 1998, 152:307-317)**

medication markedly reduces the risk for Alzheimer's disease (AD).<sup>1,2</sup> A key component of the inflammatory response in AD is the presence of activated microglia. It has been known for many years that microglia are associated with the amyloid plaque pathology in AD, but a series of more recent investigations have clearly demonstrated the presence of activated microglia.<sup>1,3,4</sup> The activated microglia are evidenced by their increased expression of various antigens, including complement receptors, major histocompatibility complex class I and class II antigens, interleukins, transforming growth factor- $\alpha$ , tyrosine kinase-related antigens such as CD45 and phosphotyrosine (PT), integrin-related receptors, and lectin-binding sites.<sup>4</sup> Activated microglia are not present in all plaques, but their presence has been correlated with the appearance of degenerating neurites,<sup>5,6</sup> apolipoprotein E, and amyloid.<sup>7,8</sup> Although the formation of fibrillar  $A\beta$  (amyloid) is thought to be mediated by  $A\beta$  neurotoxicity,<sup>9</sup> the role of the microglia in this process is unclear. Microglia may synthesize  $A\beta$ , form amyloid, clear  $A\beta$ , or play a primary or secondary role in neuron loss. Activated and proliferating microglia appear at sites of many types of neuronal damage as part of the response to injury. In most instances, their transient presence is regarded as secondary, limited, and possibly beneficial.<sup>10</sup> However, cultured microglia readily take up  $A\beta$ <sup>11,12</sup> and  $A\beta$  can increase microglial activation and neurotoxin production.<sup>13,14</sup> Thus, persistent activation of microglia associated with a protease-resistant amyloid irritant may give rise to chronic inflammation and additional tissue damage. Microglial activation may be a causal link between  $\beta$ -protein deposits and neurodegeneration leading to dementia.

Although the evidence of microglial activation associated with plaques in AD is extensive, there are only limited data from animal models where one can hope to clarify the impact of microglial activation on disease progression. Activated and  $A\beta$ -immunoreactive microglia

Supported by grants RO1 AG11125 and 5P50AG05131-13 and VA Merit (G. M. Cole) and VA Merit and grant AG10685 (S. A. Frautschy).

Accepted for publication October 17, 1997.

Address reprint requests to Dr. Greg M. Cole, Sepulveda VAMC, GRECC, 11E, 16111 Plummer Street, Sepulveda, CA 91343. E-mail: gmcole@UCLA.edu.

Epidemiological evidence from 17 different studies shows that a history of nonsteroidal anti-inflammatory

were found at early stages of plaque formation in aged primate brains.<sup>5</sup> One line of APPV717F transgenic mice developing amyloid plaques with age was previously described as having neocortex that "contained diffusely activated microglial cells, as defined by their amoeboid appearance and shortened processes." However, no figures or evidence of relationship with plaque pathology were presented.<sup>17</sup> A more extensive examination of pathology in these mice also omitted data on microglia but stated that microglial cells were associated with plaque cores and that "compared with AD" they "showed a more prominent astroglial reaction and a less abundant microglial component (not shown)." We are unaware of published data on microglia in other plaque-forming APP transgenic mice.

These observations suggested the utility of demonstrating microglial activation in an animal model for AD where a number of genetic and pharmaceutical approaches could be taken to reduce components of the microglial response and then gauge the outcome on aspects of the disease present in the model. Here we show 1) immunocytochemical evidence of a massive microglial response in plaque-forming transgenic mice and A $\beta$ 40 but not A $\beta$ 42 immunostaining of plaque microglia, 2) quantitative data linking microglial density and size to their presence in plaques, and 3) regional and layer correlations between plaques and activated microglia. These are the first quantitative data linking microglial activation to plaque formation in an animal model.

## Materials and Methods

### Animal Studies

Human APP<sup>sw</sup> transgenic mice (Tg2576) with the Swedish familial 670/671 NL double mutation under transcriptional control of the hamster prion promoter were maintained outbred to C57Bl/SJL in a standard colony and allowed to age to 10 to 16 months and develop amyloid deposits as previously described.<sup>16</sup> Surgical and animal care procedures were carried out with strict adherence to the guidelines set out in the National Institutes of Health Guide for the Care and Use of Laboratory Animals (publication 80-23).

### Antibodies

Anti-A $\beta$  antibodies used in the present study were 10G4 monoclonal to the 1 to 13 region of native human A $\beta$ 1-40<sup>17</sup>; anti-34-40 specific for A $\beta$ X-40<sup>18</sup>; affinity-purified rabbit antibody to A $\beta$ 1-5, which requires the free amino terminus of  $\beta$ 1; and affinity-purified rabbit anti-42 absorbed on A $\beta$ 43, which labels A $\beta$  peptides ending at 42 but not 43.<sup>19</sup> Additional sections were labeled with 4G8 monoclonal to A $\beta$ 17-24. All of the A $\beta$  staining reported in this paper was blockable using free peptide absorption controls on adjacent sections.<sup>17,20</sup> Monoclonal antibody to PT was from Sigma Chemical Co. (St. Louis, MO).

### Immunocytochemistry

Fourteen-micron cryostat coronal sections from hemibrains from four transgene-positive and five transgene-negative Tg2576 15- to 16-month-old mice were cut on a freezing sledge microtome from the posterior pole anteriorly through the anterior margin of the hippocampus. Fixation was by sequential immersion in 4% paraformaldehyde in PBS, followed by 50, 75, and 95% ethanol for 5 minutes each. Eight-micron paraffin coronal sections (from seven Tg2576 mice at 10 to 12 months of age) were prepared as described in Hsiao et al.<sup>16</sup> Frozen and paraffin sections were immunolabeled with anti-PT mouse monoclonal first antibody<sup>21</sup> and developed with a Vector ABC kit using biotinylated goat anti-mouse and metal-enhanced diaminobenzidine (DAB) essentially as described.<sup>17</sup> Adjacent sections were double labeled for microglia using PT (anti-mouse peroxidase/brown/DAB), followed by clearing and rehydrating to remove bound antibodies and then anti-A $\beta$  (rabbit) or 10G4 (mouse), washing, and detection with anti-rabbit or anti-mouse alkaline phosphatase with Vector blue chromophore. 10G4 was used on frozen sections unless otherwise indicated. Some sections were counterstained with contrast green (Vector Laboratories, Burlingame, CA) to locate nuclei. Congo red and thioflavin S staining was performed as previously described.<sup>16</sup>

### Lectin Staining

Biotinylated *Griffonia simplicifolia* GS b4 isolectin and antigen unmasking solution were purchased from Vector. Paraffin sections were cleared and treated with antigen unmasking solution (1:100 in distilled water) in a pressure cooker for 1 minute, washed in PBS for 5 minutes, and then treated with 0.3% hydrogen peroxide for 30 minutes to quench endogenous peroxidase. Sections were washed and then incubated overnight at 4°C with isolectin (10  $\mu$ g/ml) in 0.1% Tris-buffered saline/Tween. After washing, they were incubated with Vector ABC avidin/peroxidase complex for 45 minutes and developed with DAB. Selected sections were double labeled for A $\beta$  using Vector blue as described above.

### Image Analysis

For each section 2.5 mm posterior to Bregma ( $\pm 0.3$  mm), we examined immunohistochemical labeling in the following plaque-containing and non-plaque-containing regions: corpus callosum, hypothalamus, hilus, hippocampal fimbria, subiculum, inner and outer molecular layers of the dentate, internal capsule, lateral geniculate, entorhinal, frontal, temporal, parietal, and occipital cortex, adjacent (agranular and retrosplenial) frontal cortex, posterior thalamic nuclei, stratum oriens, stratum radiatum, and zona incerta. We also examined individual cortical layers. All histological and immunohistochemical images were acquired from an Olympus Vanox-T (AHBT) microscope with an Optronix Engineering LX-450A CCD video camera system. The video signal was then routed into a

Power Center 120 Macintosh-compatible microcomputer via a Scion Corporation AG-5 averaging frame grabber. Once digitized, the images were analyzed with NIH-Image public domain software (developed at the U.S. National Institutes of Health and available on the Internet at <http://rsb.info.nih.gov/nih-image/>). Custom Pascal macro subroutines were written and used to calculate microglial cell number per square millimeter and cell size. Each capture was exposed to the same computer subroutine to minimize biases of the microscopist; most importantly, the density slice thresholding was maintained constant throughout analysis. Running the macro resulted in images being captured in color and the appropriate slice of RGB stack being selected (green RGB slice for analysis of brown microglia), the spatial calibration being selected (magnification), the density slice to LUT (220 to 254) being set, and all of the averages and standard errors of microglia parameters being exported to an EXCEL file. Single-blind image analysis of single-labeled microglia was done with respect to transgene positivity or negativity.

Another macro measured the distribution of microglia in relation to distance from the A $\beta$ -immunoreactive plaque center. This macro involved analyzing microglial morphology in each of a series of four concentric circles within and around A $\beta$ 42-immunoreactive plaques, the ring widths of which correspond to the radii of the A $\beta$ -immunoreactive plaque (ie, the fourth circle is four plaque radii from the plaque center). Microglia parameter averages and SD of each ring were computed by Pascal subroutine and exported to EXCEL or directly to the statistics program. In this ring macro, which was used on sections double labeled for A $\beta$  (blue) and microglia (brown), the blue slice (filter) of the RGB stack was chosen and density slice threshold selected such that the blue plaque would not be picked up when imaging the brown microglia. Lack of color bleed-through was tested in singly labeled sections. As with the previous macro, all images captured for the ring macro were performed using the same density slice threshold. Statistical analysis compared transgene-positive and -negative groups or layers and regions with analysis of variance or Student's *t*-test as appropriate using SuperAnova (1.11) and StatView (4.5) for Power Macintosh.

## Results

### Identification of Plaque-Associated Microglia

GS lectin specifically labels microglia in rodent brain.<sup>22</sup> Figure 1 shows sections from APPsw transgene-positive and -negative mice labeled with biotinylated GS lectin using DAB (shown here in black) that were then photographed before double labeling with affinity-purified polyclonal antibody to the free carboxy terminus of A $\beta$ 42 using Vector Blue (shown here in gray). The antibody to A $\beta$ 42 recognizes A $\beta$  ending at amino acid 42 but not 40 or 43 (Figure 1, arrows). At low magnification, clusters of dark, lectin-labeled microglia were evident in the transgene-positive animals (Figure 1A) but not in the trans-

gene-negative controls (Figure 1B). Although small A $\beta$ 42 deposits contained only a few or no microglia in the plane of section (Figure 1C, small thick arrows), large A $\beta$ 42 deposits were associated with enlarged, darkly lectin-labeled microglia (Figure 1C, long thin arrow). Under high magnification, the deposits had clusters of lectin-stained microglia wrapping around A $\beta$ 42-labeled plaques (arrow) and neighboring cells (Figure 1D). A few vessel-associated amyloid plaques (arrow) had similar clusters of microglia (Figure 1E). In some instances, the clusters of microglia were so dense that they formed one large mass (Figure 1F). As lectin stained only cells in the plaques, we sought to obtain another method of measuring a range of microglial activation that was more amenable to quantitation as well as to strengthen the observation of microglial association with plaques.

Microglia exhibit unusually high activities of tyrosine kinases, which increase with activation,<sup>23</sup> allowing the use of PT antibodies to quantitatively assess microglial activation in the injured rodent brain.<sup>21</sup> Employing rabbit phosphotyrosine antibody to identify microglia with DAB (brown) and mouse monoclonal antibody to A $\beta$  (10G4) to label plaques (blue), we examined the association of A $\beta$  immunostaining with microglial activation.

At low power, a large number of microglial processes and enlarged microglia were found in plaque-forming areas of transgene-positive mice (Figure 2A). Much more limited, frequently vessel-associated PT labeling in the absence of plaques was found in the cortex of similarly aged transgene-negative mice (Figure 2B). This vessel labeling was consistently found in both groups and may represent perivascular microglia or a possible artifact of immersion fixation. Immunostaining for A $\beta$  alone, particularly with antibody to A $\beta$ 34-40 and A $\beta$ 1-5, showed amyloid plaques with associated cell or process labeling that was microglial-like (in Figure 2C, A $\beta$ 34-40 is indicated by arrows on the left and an arrowhead on the right). Because the A $\beta$ 34-40 antibody fails to label A $\beta$ 42 that contains the 34 to 40 peptide, this antibody should label only A $\beta$  peptides X-40 and not APP or other fragments. As previously noted, this A $\beta$ 40 antibody labeled the majority of plaques in Tg2576 mice.<sup>16</sup> Preliminary counts in 11- to 12-month-old animals show that more than 90% of the plaques are labeled by both 42- and 40-specific antibodies, but A $\beta$ 40 antibody labels larger areas. GS-lectin-labeled microglia were grossly enlarged around A $\beta$ 42-labeled amyloid and frequently wrapped around cells that were not A $\beta$ 42-positive (Figure 2D). In general, the 42 antibody did not appear to label plaque-associated processes and microglial cells even with intense DAB development in singly labeled sections. This was in contrast to antibodies recognizing A $\beta$  epitopes from  $\beta$ 1 to 40. At higher magnification, in plaque-forming regions, enlarged PT-labeled microglia often co-stained for A $\beta$  (10G4) and extended their processes around adjacent unstained cells (black, open arrow in Figure 2E). Intensely labeled amoeboid microglial cells and their processes were in and adjacent to the plaques (Figure 2, F and G). In Figure 2G, three examples of vessel-associated microglia are shown (arrows). The microglia appear to be clustering around patches of A $\beta$  immunostaining

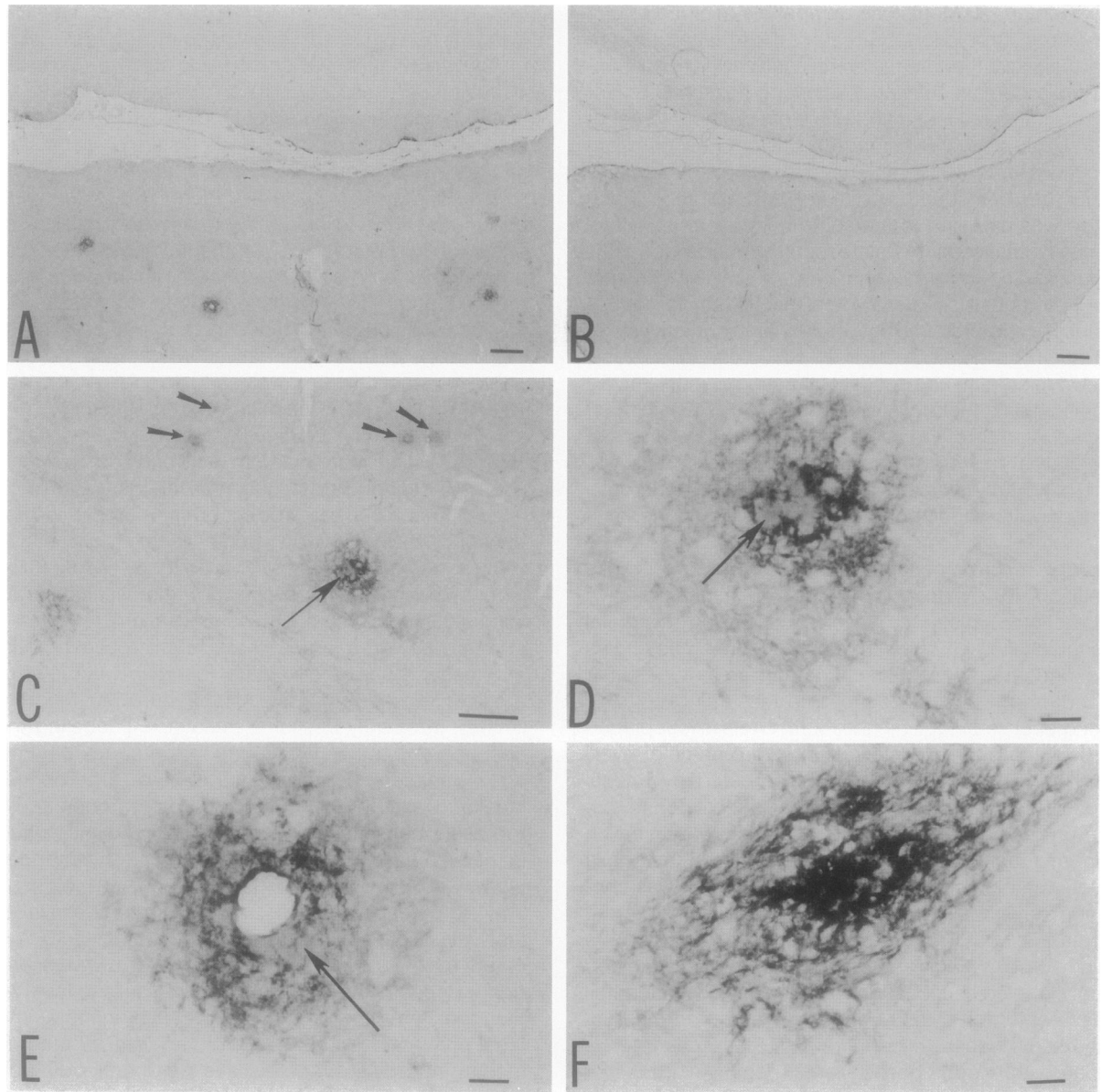


**Figure 1.** Relationship between  $A\beta$  immunostaining and microglia. Microglia are identified with GS lectin labeling (stained with DAB, brown, shown here as black) and plaques by  $A\beta_{42}$  immunostaining (stained blue, shown here as gray with arrows). **A** and **B**: Transgene-positive mice (**A**) reveal large clusters of microglia in coronal sections, but transgene-negative mice (**B**) do not. **C**: At intermediate magnification in the occipital cortex and presubiculum, small  $A\beta_{42}$ -positive plaques contained few or no lectin-stained microglia (**thick arrows**) whereas large plaques contained prominent plaque-associated masses of lectin labeling (**thin arrow**). **D**: Higher magnification of plaque in **C**. The Vector Blue- $A\beta$ -stained amyloid core (**arrow**) is surrounded by intensely DAB-labeled, lectin-positive microglia (black). **E**: A similar cluster of microglia (black) around perivascular amyloid (**arrow**) in the subiculum. **F**: Cortical plaque with very dramatic massing of lectin-stained microglia (black). Bars, 200  $\mu\text{m}$  (**A** and **B**), 100  $\mu\text{m}$  (**C**), and 20  $\mu\text{m}$  (**D** to **F**).

(Figure 2F). Sometimes the PT-positive amoeboid microglia encircled a central amyloid core (light blue, Figure 2H) or massed over the entire plaque and were both PT and  $A\beta$  positive (black, Figure 2H, inset). The black double labeling seen in the inset and in Figure 2E could represent  $A\beta$  in or on the surface of microglia.

In a previous study,<sup>16</sup> we showed that the plaques labeled with Congo red and thioflavin S. Preliminary data counting 4G8-labeled plaques on adjacent sections show that roughly 50% of the neocortical and limbic deposits are Congo red-positive and 80% are thioflavin

S-positive, indicating the presence of amyloid fibrils in the majority of plaques.

Because of the high resolution of individual cells with PT, we used PT immunostaining for quantitative morphometric studies of microglia using NIH Image. The average density and cell area of PT-labeled microglia in 18 regions of coded coronal sections (defined below) was determined, and then all data were assigned to transgene-positive and -negative groups. Microglia density (number of PT-labeled cells per square millimeter) for all areas was significantly increased ( $P < 0.01$ ) in the trans-

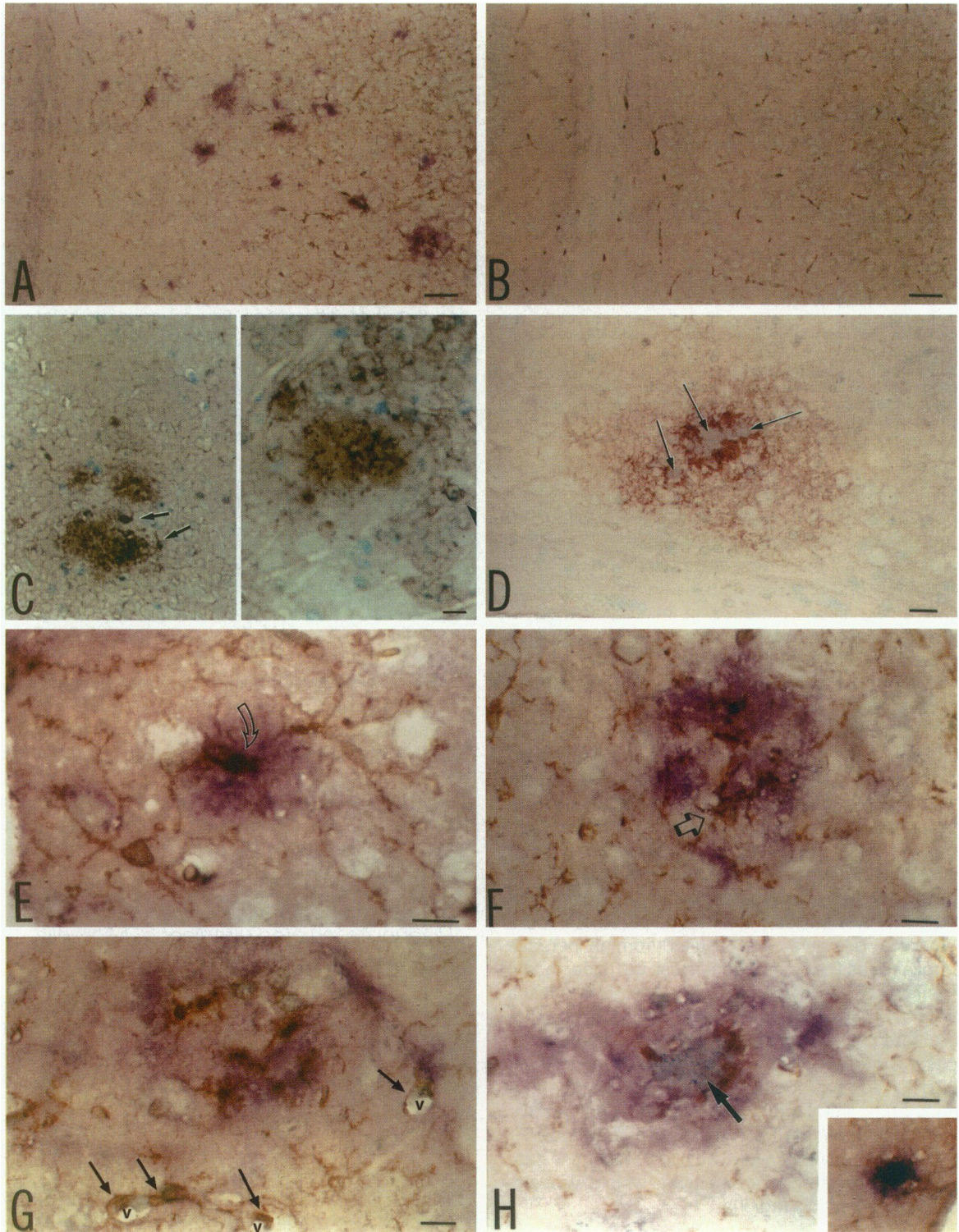


**Figure 2.** Relationship between  $A\beta$  immunostaining and microglia. **A:** Several  $A\beta$ -positive plaques (10G4, blue) containing large immunopositive phosphotyrosine-labeled microglia (PT, brown) in transgene-positive mice in addition to PT labeling of vessels not associated with plaques. **B:** PT labeling (brown) in the absence of plaques (10G4, blue) in cortex of similarly aged transgene-negative mice is vessel associated and devoid of large microglia. **C:** Singly stained sections with anti- $A\beta_{34-40}$  ( $A\beta_{40}$  specific, brown) in cortex reveal cells with microglial morphology on the right (arrows) and, on the left small basophilic (contrast green) nuclei (arrowhead). **D:** The GS lectin-labeled microglia (brown) were grossly enlarged around  $A\beta_{42}$ -specific immunostaining (blue) and frequently wrapped around cells in the adjacent area. **E:** Enlarged PT-labeled microglia (brown) in plaque-forming regions (10G4, blue) with processes encircling a neuron as well as apparent co-localization of 10G4 and PT immunostaining to produce black (open arrow). **F:** PT-positive microglia (brown) massing (open arrow) around patches of  $A\beta$  immunostaining (10G4, blue). **G:** PT-labeled amoeboid microglia clustered around a plaque (10G4, blue) and examples of microglia (brown, arrows) associated with vessels (v). **H:** PT-positive amoeboid microglia (brown) encircling a central amyloid core (10G4, blue) or (inset) microglia massed over another plaque that is both PT and  $A\beta$  positive (black). Bars, 100  $\mu\text{m}$  (A), 50  $\mu\text{m}$  (B), 30  $\mu\text{m}$  (C, right), 20  $\mu\text{m}$  (C, left, and D), and 10  $\mu\text{m}$  (E to H).

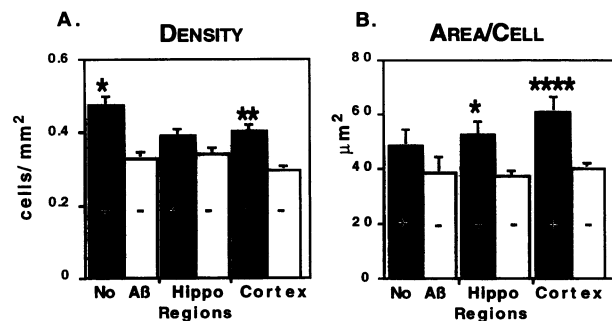


**Figure 3.** Regional analysis of microglial morphology. We compared transgene-positive with transgene-negative mice in three grouped regions (two plaque-containing regions, hippocampus and cortex, and one non-plaque-containing region, thalamus) for microglia density (A) and microglia area/cell (B). Differences between transgene-positive and -negative mice in non-plaque-containing areas were observed only for density. This was due to differences mainly in the lateral geniculate body, which innervates the occipital cortex, a high plaque-containing region. Differences in area/cell between transgene-positive and -negative mice were significant only in plaque-containing regions, the hippocampus and cortex. Error bars show SEM: \* $P < 0.05$ ; \*\* $P < 0.01$ ; \*\*\* $P < 0.001$ , \*\*\*\* $P < 0.0001$ .

gene-positive sections as was total area/microglia ( $P < 0.001$ ; not shown). A more detailed analysis of PT staining in each of the 18 different regions was performed (Figure 3). Orthogonal comparisons within the same region demonstrated a significant increase in microglial area in transgene-positive compared with transgene-negative mice in parietal ( $P < 0.05$ ), temporal ( $P < 0.05$ ), entorhinal ( $P < 0.001$ ), and stratum oriens of the hippocampus ( $P < 0.05$ ; not shown). As multiple comparisons increase the chance of a type II error, additional regional analysis involved grouping regions in terms of plaque-containing (hippocampus or cortex) and non-plaque-containing regions and making minimal planned orthogonal comparisons only between the microglia parameters in transgene-positive and -negative mice within these three regions (Figure 3, A and B). In non-plaque-containing areas, transgene-positive and -negative mice were not significantly different, except for a single parameter, density ( $P < 0.05$ ). This difference resulted from an increase in microglia density of transgene-positive mice in the lateral geniculate, which projects to the occipital cortex, a high plaque region. In the plaque-containing region, the cortex, differences in microglial density between transgene-positive and -negative mice were highly significant ( $P < 0.01$ ). Also, in plaque-containing regions (the hippocampus and cortex) there was a significant difference in the microglia area/cell. This quantitative analysis of PT is consistent with a subjective evaluation of the less sensitive microglia marker, lectin staining, which was elevated in plaque-forming regions.

### Effect of Transgene on Microglia and Plaques in Cortical Layers

The density of plaques showed a layer-dependent distribution in the neocortex (not shown). Plaque density was highest in layer I, intermediate in layers II to IV, and significantly lower in layers V and VI ( $P < 0.05$ ; not shown). Therefore, we analyzed the possibility of a layer

effect in microglia parameters in adjacent sections stained singly for PT. Although analysis of microglial parameters showed no layer effect in transgene-negative animals, in transgene-positive animals, microglial density was highest in layer 1 of the neocortex, intermediate in layers 2 to 4, and lowest in layers 5 and 6 (not shown). Similar results showing significant differences between layers within the transgene-positive mice were found with microglial area ( $P < 0.05$ ; data not shown). Orthogonal comparisons were also made between transgene-positive and -negative mice within a region. Highly significant differences were found between the positive and negative groups in the layers with the most plaques (layers 1 to 4), but no differences were found in the layers with the fewest plaques (layers 5 and 6) in microglial density and area (not shown). Regional differences in microglia parameters in cortical layers were most prominent and highly significant in the entorhinal cortex, one of the regions with the highest number of plaques (not shown).

### Regional Plaque Distribution

Plaque density and diameter was determined across brain regions in sections adjacent to those used for microglial morphometry. Plaques were found throughout the neocortex and hippocampus but not in other regions examined (not shown). The highest plaque numbers were in entorhinal and occipital cortex and hippocampus. The average plaque diameter was significantly larger in the frontal and adjacent (retrosplenial and agranular) cortex where plaques were fewer in number (not shown). These results reflect plaque distribution in adjacent sections that were analyzed for microglial morphometry but do not necessarily represent overall regional differences in plaque numbers. Those data require the complete stereological analysis of plaques through serially sectioned brain.<sup>24</sup>

### Plaque-Associated Gradient of Microglia Parameters

To test the hypothesis that microglial activation was closely linked to A $\beta$  deposition, sections were double labeled for A $\beta$  (blue) and PT (brown) as in Figure 2, and PT-labeled microglia were quantitated in four concentric rings centered on plaques as a function of the distance from the center of the plaque (Figure 4A). The first ring included the A $\beta$ -stained area (plaque) whereas rings 2 to 4 each extend one additional plaque radius from the center so that the outside of the largest ring is four plaque radii from the center. Within plaques there is a highly significant three- to fivefold increase in microglial cells per square millimeter (Figure 4B) and area/cell (Figure 4C) with a continuing reduction in density in the outer rings ( $P < 0.001$ ). Density in ring 2 just outside the plaque was higher than in ring 4 ( $P < 0.05$ ; Figure 4B).

As the size of rings depended on plaque size, we also performed regression analysis to calculate the regression of microglial parameters on distance from the core of the plaque, regardless of plaque size. Consistent with the

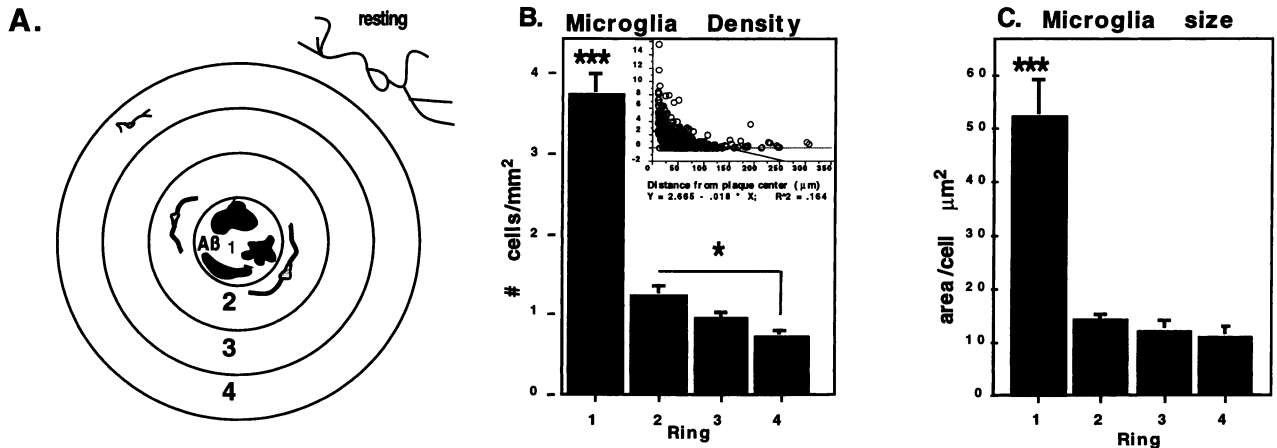


**Figure 4.** Microglial density and morphology in relation to plaque distance. Sections were double stained: brown for microglia with PT antibody and blue for A $\beta$  using anti-A $\beta$ 1-5. **A:** Image analysis method showing four rings in which microglia parameters were quantified for each A $\beta$  deposit. Ring 1 measurements represent microglia parameters within the entire plaque stained for A $\beta$ . Rings 2 to 4 are each the width of one plaque radius. **B:** All microglia parameters were statistically analyzed by analysis of variance as a function of distance from plaque center. Microglia density within the plaque was significantly higher than in rings 2 to 4 ( $P < 0.001$ ), and ring 2 was higher than ring 4 ( $P < 0.05$ ). **B, inset:** Regression analysis is shown as a function of distance from plaque center (ring radius). Microglial density decreased as a function of distance from the A $\beta$  core ( $P < 0.0001$ ) using either a linear regression (shown) or polynomial fit. The equation for the polynomial fit is  $y = 4.03 - 0.061x + 1.951 \times 10^{-4} x^2$ ;  $R^2 = 0.307$ ;  $*P < 0.05$ ;  $***P < 0.001$ . **C:** Microglia within the A $\beta$  plaque were larger ( $P < 0.001$ ) than outside the plaque.

ring analysis, there was a rapid and highly significant ( $P < 0.0001$ ) decrease in microglial density ( $y$ ) as distance ( $x$ ) from the plaque center moved from 0  $\mu\text{m}$  (plaque center) to 400  $\mu\text{m}$  distally with linear ( $y = 2.745 - 0.14x$ ) or polynomial regression ( $P < 0.0001$ ;  $y = 4.03 - 0.061x + 1.951 \times 10^{-4} x^2$ ; Figure 4B, inset). The 2.9% of all plaques that had no PT-stained microglia are indicated by rings with microglia averaging zero. As with most markers for microglial antigens, the amount of PT is proportional to state of activation. As only 50 to 80% of the plaques had Congo-red- or thioflavin-S-positive amyloid, it is clear that diffuse deposits also contained PT-stained microglia. Specific examples of diffuse A $\beta$  immunostaining and morphologically activated microglia were observed (consisting of enlarged, shortened, thickened processes, approaching amoeboid shape), but the vast majority of fully activated, amoeboid microglia were associated with cored plaques.

## Discussion

### Parallels to Alzheimer's Brain

Our results show strong qualitative evidence of microglial activation using both lectin and PT staining and quantitative evidence of microglial activation in plaque-forming areas of mice carrying the HuAPPsw transgene relative to their nontransgenic littermates. These mice show a 4 to 8% neocortical amyloid burden at 16 months, which is comparable to that seen in human AD.<sup>24</sup> The majority of the deposits contain fibrillar amyloid. Regional analysis of microglia in association with plaque density and size (see Results) suggests that the altered microglial morphology associated with the expression of the transgene results from A $\beta$  deposition and not from other effects of APP expression. Together, these results show an overall increase in microglial density and size in the transgenic

animals that correlates qualitatively and quantitatively with plaque distributions. That is, activation of microglia as indexed by their increased density and size occurred primarily in regions with A $\beta$  deposit formation, particularly the entorhinal and occipital cortex and hippocampal formation.

Similar to reports on AD brain,<sup>4</sup> clusters or even masses of activated microglia were found associated with plaques in all regions of the neocortex and in the hippocampus. The enlarged, amoeboid microglia in and around plaques of the transgenic mouse (as shown in Figures 1 and 2) are very similar to AD brain.<sup>25-27</sup> In particular, the microglia encircling but not entering amyloid cores (Figure 2H) represents a classical configuration demonstrated in ultrastructural images of AD brain.<sup>28,29</sup> However, even at the ultrastructural level, microglial processes interdigitate with the amyloid fibrils in AD, and it is frequently difficult to determine whether the A $\beta$  is inside or outside of cells. Therefore, apparent microglia double labeling with A $\beta$  at the light level can only confirm a close association but does not imply intracellular microglial A $\beta$  or amyloid.

Ring analysis confirmed the spatial link between A $\beta$  deposits and microglia that was implicated by microglial analysis of singly PT-stained sections. Furthermore, this analysis demonstrates that shrinking of cells occurs farther away from the core, suggesting that cells are activated within the core. This is illustrated by the qualitative morphological observation in Figures 1 and 2 demonstrating that, within the plaque core, the microglia were enlarged with thickened, shorter processes.

A predilection for plaques in specific layers of occipital cortex<sup>30</sup> and an association of plaques with specific cortical layers have also been reported in AD brain.<sup>31,32</sup> Most analyses have focused on the laminar distribution of neuritic plaques, especially in neocortical layers II and III using silver stains or thioflavin-positive amyloid in specific

regions of the hippocampus (eg, molecular layer of the dentate) or cortex. More recently, with A $\beta$  labeling in AD temporal cortex, area 22, densities of stellate and diffuse deposits were found to be highest in layers I, III, and IV.<sup>32</sup> Another study (using quantitative image analysis) examined the laminar distribution of A $\beta$  staining in prefrontal cortex of AD cases and found that the majority of deposits (classified as punctate and macular) were in layers I to III with most of the punctate (~9  $\mu$ m diameter) deposits in layer I.<sup>33</sup> The A $\beta$ -rich layer I contains large numbers of distal apical dendrites and associative axon projections in contrast to A $\beta$ -poor layer VI.<sup>33</sup> A $\beta$  immunostaining on the surfaces of apical dendrites at apparently early stages of amyloid deposition has been reported in cross-sectional studies,<sup>34</sup> and A $\beta$  deposits have been observed to be in between apical dendrites of pyramidal cells.<sup>35</sup> The laminar organization of A $\beta$  deposits we observed in the transgenic mice is thus in general agreement with observations on AD tissue and consistent with the high level of transgene expression in neurons and a neuronal source (or sink) for the deposited A $\beta$ .

The observed association of activated microglia with plaques could reflect a response to amyloid or injury or both. One would expect a response to amyloid based on studies with cultured cells where A $\beta$  peptide alone can activate microglia.<sup>36</sup> Although dystrophic neurites occur in Tg2576 mice by 15 to 16 months of age, there is no evidence of major synapse and neuron loss in the regions examined<sup>24</sup> in contrast to the damage found in postmortem AD brain where significant neuron loss occurs. In the outer molecular layer of the dentate gyrus of AD brain, activated microglia appear to be increased in both plaque and nonplaque regions, consistent with responses to neuronal injury as well as amyloid.<sup>26</sup>

### *Response to Injury*

Although most of the microglial activation occurred in plaque-forming areas in the Tg2576 APPsw mice, a trend toward increased activation in some areas lacking A $\beta$  deposits (especially the lateral geniculate that projects to the occipital cortex, a high plaque-containing region) also occurred, consistent with a response to injury in these regions. However, we have no direct evidence of injury in these areas. Perineuronal microglia with processes encircling neurons have been frequently observed in electron micrographs of damaged brain.<sup>10</sup> GS lectin labeling revealed many examples of microglial processes encircling large cells in the immediate vicinity of plaques (Figures 1 and 2), consistent with an injury process. Unlike the 1-year-old Tg2576 mouse, postmortem AD brain typically involves significant neuron loss and large numbers of tangle-bearing neurons. This injury would be expected to provoke microglial activation far from A $\beta$  deposits and weaken the correlation with plaques.

### *A $\beta$ Immunostaining of Microglia*

As illustrated in Figure 2, we found immunostaining of plaque-associated cells with small basophilic nuclei and

microglial morphology with antibodies to A $\beta$ 1–5, A $\beta$ 5–13 (10G4), and A $\beta$ 34–40 but not with antibody for the free carboxy terminus of A $\beta$ 42. We also found them with 4G8 (not shown). Some plaque-associated microglia were also A $\beta$  immunopositive. Because the A $\beta$ 40 and A $\beta$ 42 immunostaining requires the free carboxy terminus of A $\beta$ , they are the most appropriate probes to distinguish A $\beta$ X–40 and A $\beta$ X–42 from cellular APP fragments that include the A $\beta$  domain. However, even at the ultrastructural level, investigators have had difficulty in telling whether fibrils are inside or out. With the methods used, it is impossible to distinguish intracellular from surface A $\beta$  or closely associated extracellular A $\beta$  immunostaining. We do not know why the A $\beta$ 40 but not the A $\beta$ 42 antibody labeled microglia, but this result is intriguing. Antibodies from  $\beta$ 1 to  $\beta$ 40 also labeled more diffuse material around plaques than the 42-specific antibody (not shown). One possibility is that microglia may scavenge diffusely distributed A $\beta$ 40 and compact it. Intriguingly, two previous reports have found that A $\beta$ 40-positive plaques in AD brain contained compacted amyloid and were selectively associated with microglia.<sup>25,37</sup> The published enzyme-linked immunosorbent assay data on the HuAPPsw Tg2576 mice showed that 60% of the total A $\beta$  at 11 to 12 months was A $\beta$ 40,<sup>16</sup> consistent with the marked microglial response in these mice. The majority of deposits had microglia and stained for A $\beta$ 40. This is in contrast to the APP717F mouse where the A $\beta$  in aged brains is 89 to 99% A $\beta$ 42<sup>38</sup> and there are fewer microglia than in AD cases.<sup>39</sup> AD cases with APP717 mutations typically have more A $\beta$ 42 than sporadic AD or APP670/671 cases.<sup>40</sup> The percentage of A $\beta$ 40 varies with disease progression and apolipoprotein (Apo)E genotype. Because ApoE4, which is known to accelerate disease onset, specifically increases the percentage of A $\beta$ 40 and not A $\beta$ 42,<sup>41,42</sup> the link between A $\beta$ 40 and microglia may be relevant not only to plaque progression but also to clinical onset. Microglia make and take up ApoE and are the major ApoE-positive cells in plaques.<sup>7</sup> ApoE-positive, plaque-associated cells resembling microglia were also found in Tg2576 mice (not shown).

### *Microglial Interactions with A $\beta$ in Culture and after Brain Infusion*

Possible roles for microglia interacting with A $\beta$  in plaques have been identified *in vitro*. Microglia readily take up and either accumulate or degrade A $\beta$  in culture.<sup>11,12</sup> Two microglial receptors for A $\beta$  have been recently reported, a scavenger receptor for fibrils<sup>43,44</sup> and the RAGE receptor for soluble A $\beta$ .<sup>45</sup> Either of these or other receptors for ApoE lipoproteins that carry A $\beta$  may regulate A $\beta$ -microglial interactions, leading to their activation and secretion of interleukin-1 $\beta$ , tumor necrosis factor- $\alpha$ , nitric oxide, superoxide radical, hydrogen peroxide, and other potent cytokines and toxins.<sup>4</sup> Interleukins have a major impact on astrocyte functions, including ApoE synthesis.<sup>8</sup> *In vitro*, secretion of microglial neurotoxins has been shown to increase when the cells are fed A $\beta$ , and the increased neurotoxicity of media from these cultures has been dem-



onstrated.<sup>14,36</sup> We have shown that injection of peptides capable of modulating the microglial response, including macrophage inhibitory factor and tuftsin also influence deposit formation with intraventricularly infused A $\beta$ .<sup>46</sup> Activated microglia also produce and secrete transforming growth factor (TGF)- $\beta$ 1 *in vitro* and appear to be a major TGF- $\beta$ 1 source in injured brain.<sup>47</sup> When TGF- $\beta$ 1, a potent regulator of microglial activation, was co-injected with the infused A $\beta$ 40 peptide, widely distributed, thioflavin-S-positive amyloid plaques and clusters of microglia formed between the ventricle and the TGF- $\beta$ 1 injection site.<sup>48</sup> Therefore, interleukins and TGF- $\beta$  secreted by activated microglia could have a significant impact on plaque progression leading to ApoE-dependent A $\beta$ 40 deposition. These data provide additional support for a microglial role in plaque pathogenesis related to deposit formation.

### *Microglia and Plaque Progression*

Like dystrophic neurites, the presence of activated microglia in plaques in AD brain has been linked to the presence of  $\beta$ -amyloid. In the Dutch-type cerebrovascular amyloidosis, there are parenchymal A $\beta$  deposits that lack amyloid, dystrophic neurites, and microglia.<sup>49</sup> Similarly, pure diffuse A $\beta$  deposits in dorsal striatum lack amyloid, dystrophic neurites, ApoE, and activated microglia.<sup>50,51</sup> Conversely, white matter  $\beta$ -amyloid deposits were found to lack reactive astrocytes or abnormal neuronal components but were consistently linked to aggregates of activated microglia.<sup>52</sup> Another study quantified microglial density in three groups: 1) aged, nondemented brains with only diffuse plaques, 2) aged, nondemented brains with both diffuse and neuritic plaques, and 3) AD patients with all types of plaques. The comparison revealed an increase in the mean density of microglia in AD brain and a close association with neuritic but not diffuse plaques.<sup>27</sup> Given that analysis of serial sections shows two to five times more classic plaques than single sections,<sup>53</sup> reports of activated microglia in the majority of diffuse deposits without neurites<sup>6</sup> may be missing neurites and amyloid in neighboring sections. The same phenomena may lead to an overestimation of activated microglia in apparent diffuse plaques in our transgenic mice. This seems highly likely given that, although there is an exponential drop in microglial density away from the plaque center in the mouse, microglial density as far as 100 to 150  $\mu$ m from the plaque core is still moderately increased (Figure 2B, inset). In other studies of AD brain, interleukin-1 $\alpha$ -positive (activated) microglia were correlated with the presence of dystrophic neurites<sup>6</sup> and ApoE.<sup>8</sup> This correlation between activated microglia and ApoE immunostaining of deposits was attributed to interleukin-stimulated astroglial synthesis of ApoE. However, as stated previously, another report suggests that microglia and not astrocytes are ApoE immunoreactive in and around plaques in AD brain.<sup>7</sup> Both direct and indirect microglial effects involving ApoE may occur leading to isoform-dependent A $\beta$ 40 deposition.

The good correlation between neuritic plaques and activated microglia may be clinically significant because

neuritic plaque counts have a much better correlation with dementia than total plaque counts.<sup>54</sup> Comparison of brains from clinically normal individuals with high plaque counts and brains from AD patients revealed fewer activated microglia in the nondemented group and that synapse loss and dementia correlated with activation of complement and microglia.<sup>55</sup> A similar comparison found that high-plaque, nondemented brains had fewer neuritic plaques with activated microglia than AD cases,<sup>56</sup> consistent with an important role for microglial activation in neurodegeneration and clinical progression.

Available human pathology data reveal a strong correlation between microglial activation and the progression from preamyloid or pure diffuse deposits to neuritic or classical plaques with more compacted amyloid, A $\beta$ 40, abnormal neurites, and ApoE. This pathological progression appears related to the development of dementia. However, none of the correlative data can explain whether the microglial activation occurs as a cause or consequence of the abnormal neurites, amyloid fibrils, or ApoE associated with more mature plaques. Data with silver stains and with confocal synaptophysin/A $\beta$  double labeling show that Tg2576 APPsw mice at 16 months appear to have dystrophic neurites in a subset of plaques.<sup>24</sup> Furthermore, at 11 to 12 months, staining for highly phosphorylated tau with the antibody AT8 revealed that 30% of plaques analyzed contained dystrophic neurites (unpublished observations).

In summary, these mice show significant microglial activation that correlates with plaque density, plaque size, and plaque region. Furthermore, within each plaque there is a significant gradient of microglial activation that decreases with distance away from the center. These data support the hypothesis that microglial activation is a response to A $\beta$  deposition that could lead to neuritic plaque formation in a rodent model of Alzheimer's. Thus, these mice are a suitable model for ongoing experiments designed to target the microglia, block their activation, and determine the consequences related to plaque pathogenesis, dystrophic neurite formation, and memory deficits.

### *Acknowledgments*

We are grateful to the Thomas E. and Elizabeth Plott family for their support. We acknowledge the helpful comments of Dr. Bruce Teter, Dr. Marni Harris, and Jason Sigel in reviewing the manuscript. We thank Ping Ping Chen for technical assistance.

### *References*

1. McGeer PL, Schulzer M, McGeer EG: Arthritis and anti-inflammatory agents as possible protective factors for Alzheimer's disease: a review of 17 epidemiologic studies. *Neurology* 1996, 47:425-432
2. Stewart WF, Kawas C, Corrada M, Meter EJ: Risk of Alzheimer's disease and duration of NSAID use. *Neurology* 1997, 48:626-632
3. Eikelenboom P, Zhan SS, Van Gool WA, Allsop D: Inflammatory mechanisms in Alzheimer's disease. *Trends Pharmacol Sci* 1994, 15:447-450
4. McGeer PL, McGeer EG: The inflammatory response system of brain:

- implications for therapy of Alzheimer and other neurodegenerative diseases. *Brain Res Rev* 1995, 21:195-218
5. Martin LJ, Pardo CA, Cork LC, Price DL: Synaptic pathology and glial responses to neuronal injury precede the formation of senile plaques and amyloid deposits in the aging cerebral cortex. *Am J Pathol* 1994, 145:1358-1381
  6. Griffin WS, Sheng JG, Roberts GW, Mrak RE: Interleukin 1 expression in different plaque types in Alzheimer's disease: significance in plaque evolution. *J Neuropathol Exp Neurol* 1995, 54:276-281
  7. Uchihara T, Duyckaerts C, He Y, Kobayashi K, Seilhean D, Amouyel P, Hauw J-J: ApoE immunoreactivity and microglial cells in Alzheimer's disease brain. *Neurosci Lett* 1995, 195:5-8
  8. Sheng JG, Mrak RE, Griffin WS: Apolipoprotein E distribution among different plaque types in Alzheimer's disease: implications for its role in plaque progression. *Neuropathol Appl Neurobiol* 1996, 22:334-341
  9. Pike CJ, Burdick D, Walencewicz AJ, Glabe CG, Cotman CW: Neurodegeneration induced by  $\beta$ -amyloid peptides in vitro: the role of peptide assembly state. *J Neurosci* 1993, 13:1676-1687
  10. Kreutzberg GW: Microglia, the first line of defence in brain pathologies. *Arzneimittel-Forschung* 1995, 45:357-360
  11. Ard MD, Cole GM, Wei J, Mehrle AP, Fratkin JD: Scavenging of Alzheimer's amyloid  $\beta$ -protein by microglia in culture. *J Neurosci Res* 1996, 43:190-202
  12. Shaffer LM, Dority MD, Gupta-Bansal R, Frederickson RC, Younkin SG, Brunden KR: Amyloid  $\beta$  protein removal by neuroglial cells in culture. *Neurobiol Aging* 1995, 16:737-745
  13. Klegeris A, Walker DG, McGeer PL: Activation of macrophages by Alzheimer  $\beta$  amyloid peptide. *Biochem Biophys Res Commun* 1994, 199:984-991
  14. Giulian D, Haverkamp LJ, Yu JH, Karshin W, Tom D, Li J, Kirkpatrick J, Kuo LM, Roher AE: Specific domains of  $\beta$ -amyloid from Alzheimer plaque elicit neuron killing in human microglia. *J Neurosci* 1996, 16:6021-6037
  15. Games D, Adams D, Alessandrini R, Barbour R, Berthelette P, Blackwell C, Carr T, Clemens J, Donaldson T, Gillespie F, Guido T, Hago-plan S, Johnson-Wood K, Khan K, Lee M, Leibowitz P, Lieberburg I, Little S, Masliah E, McConlogue L, Montoya-Zavala M, Mucke L, Paganini L, Penniman E, Power M, Schenk D, Seubert P, Snyder B, Soriano F, Tan H, Vitale J, Wadsworth S, Wolozin B, Zhao J: Alzheimer-type neuropathology in transgenic mice overexpressing V717F  $\beta$ -amyloid precursor protein. *Nature* 1995, 373:523-527
  16. Hsiao K, Chapman P, Nilsen S, Eckman C, Harigaya Y, Younkin S, Yang F, Cole G: Correlative memory deficits,  $A\beta$  elevation and amyloid plaques in transgenic mice. *Science* 1996, 274:99-102
  17. Yang F, Mak K, Vinters HV, Frautschy SA, Cole GM: Monoclonal antibody to the C-terminus of  $\beta$ -amyloid. *Neuroreport* 1994, 15:2117-2120
  18. Mak K, Yang F, Vinters HV, Frautschy SA, Cole GM: Polyclonals to  $\beta$ -amyloid (1-42) identify most plaque and vascular deposits in Alzheimer cortex, but not striatum. *Brain Res* 1994, 667:138-142
  19. Saido TC, Iwatsubo T, Mann DMA, Shimada H, Ihara Y, Kawashima S: Dominant and differential deposition of distinct  $\beta$ -amyloid peptide species,  $A\beta$ N3(PE) in senile plaques. *Neuron* 1995, 14:457-466
  20. Cole GM, Masliah E, Shelton ER, Chan HW, Terry RD, Saitoh T: Accumulation of amyloid precursor protein fragment in Alzheimer plaques. *Neurobiol Aging* 1991, 12:85-91
  21. Korematsu K, Goto S, Nagahiro S, Ushio Y: Microglial response to transient focal cerebral ischemia: an immunocytochemical study on the rat cerebral cortex using anti-phosphotyrosine antibody. *J Cereb Blood Flow Metab* 1994, 14:825-830
  22. Kato H, Kogure K, Araki T, Itoyama Y: Graded expression of immunomolecules on activated microglia in the hippocampus following ischemia in a rat model of ischemic tolerance. *Brain Res* 1995, 694:85-93
  23. Karp HL, Tillotson ML, Soria J, Reich C, Wood JG: Microglial tyrosine phosphorylation systems in normal and degenerating brain. *Glia* 1994, 11:284-290
  24. Irrizarry MC, McNamara M, Fedorchak K, Hsiao K, Hyman BT: APPsw transgenic mice develop age-related  $A\beta$  deposits and neuropil abnormalities, but no neuronal loss in CA1. *J Neuropathol Exp Neurol* 1997, 56:965-973
  25. Fukumoto H, Asami-Odaka A, Suzuki N, Iwatsubo T: Association of  $A\beta$  40-positive senile plaques with microglial cells in the brains of patients with Alzheimer's disease and in non-demented aged individuals. *Neurodegeneration* 1996, 5:13-17
  26. Roe MT, Dawson DV, Hulette CM, Einstein G, Crain BJ: Microglia are not exclusively associated with plaque-rich regions of the dentate gyrus in Alzheimer's disease. *J Neuropathol Exp Neurol* 1996, 55:366-371
  27. MacKenzie IR, Hao C, Munoz DG: Role of microglia in senile plaque formation. *Neurobiol Aging* 1995, 16:797-804
  28. Wisniewski HM, Weigel J, Wang KC, Kujawa M, Lach B: Ultrastructural studies of the cells forming amyloid fibers in classical plaques. *Can J Neurol Sci* 1989, 16:535-542
  29. Wisniewski HM, Weigel J: The role of microglia in amyloid fibril formation. *Neuropathol Appl Neurobiol* 1994, 20:192-194
  30. Braak H, Braak E, Kalus P: Alzheimer's disease: area 1 and laminar pathology in the occipital isocortex. *Acta Neuropathol* 1989, 77:494-506
  31. Rafalowska J, Barcikowska M, Wen GY, Wisniewski HM: Laminar distribution of neuritic plaques in normal aging, Alzheimer's disease and Down's syndrome. *Acta Neuropathol* 1988, 77:21-25
  32. Delaere P, Duyckaerts C, He Y, Piette F, Hauw JJ: Subtypes and differential laminar distributions of  $\beta$  A4 deposits in Alzheimer's disease: relationship with the intellectual status of 26 cases. *Acta Neuropathol* 1991, 81:328-335
  33. Majocha RE, Benes FM, Reifel JL, Rodenrys AM, Marotta CA: Laminar-specific distribution and infrastructural detail of amyloid in the Alzheimer disease cortex visualized by computer-enhanced imaging of epitopes recognized by monoclonal antibodies. *Proc Natl Acad Sci USA* 1988, 85:6182-6186
  34. Probst A, Langui D, Ipsen S, Robakis N, Ulrich J: Deposition of  $\beta$ /A4 protein along neuronal plasma membranes in diffuse senile plaques. *Acta Neuropathol* 1991, 83:21-29
  35. Kosik KS, Rogers J, Kowall NW: Senile plaques are located between apical dendritic clusters. *J Neuropathol Exp Neurol* 1987, 46:1-11
  36. Meda L, Cassatella MA, Szendrel GI, Otvos L, Baron P, Villalba M, Ferrai D, Rosl F: Activation of microglial cells by  $\beta$ -amyloid protein and interferon- $\gamma$ . *Nature* 1995, 347:647-650
  37. Mann DM, Iwatsubo T, Fukumoto H, Ihara Y, Odaka A, Suzuki N: Microglial cells and amyloid  $\beta$  protein ( $A\beta$ ) deposition: association with  $A\beta$  40-containing plaques. *Acta Neuropathol* 1995, 90:472-477
  38. Johnson-Wood K, Lee M, Motter R, Hu K, Gordon G, Barbour R, Khan K, Gordon M, Tan H, Games D, Lieberburg I, Schenk D, Seubert P, McConlogue L: Amyloid precursor protein processing and  $A\beta$ 42 deposition in a transgenic mouse model of Alzheimer disease. *Proc Natl Acad Sci USA* 1997, 94:1550-1555
  39. Masliah E, Sisk A, Mallory M, Mucke L, Schenk D, Games D: Comparison of neurodegenerative pathology in transgenic mice overexpressing V717F  $\beta$ -amyloid precursor protein and Alzheimer's disease. *J Neurosci* 1996, 16:5795-5811
  40. Mann DMA, Iwatsubo T, Ihara Y, Cairns NJ, Lantos PL, Bogdanovic N, Lannfelt L, Winblad B: Predominant deposition of amyloid- $\beta$ 42(43) in plaques in cases of Alzheimer's disease and hereditary cerebral hemorrhage associated with mutations in the amyloid precursor protein gene. *Am J Pathol* 1996, 148:1257-1266
  41. Ishii K, Tamaoka A, Mizusawa H, Shoji S, Ohtake T, Fraser PE, Takahashi H, Tsuji S, Gearing M, Mizutani T, Yamada S, Kato M, St George-Hyslop PH, Mirra SS, Mori H:  $A\beta$ 1-40 but not  $A\beta$ 1-42 levels in cortex correlate with apolipoprotein E E4 allele dosage in sporadic Alzheimer's disease. *Brain Res* 1997, 748:250-252
  42. Mann DMA, Iwatsubo T, Pickering-Brown SM, Owen F, Saido TC, Perry RH: Preferential deposition of amyloid  $\beta$  protein ( $A\beta$ ) in the form of  $A\beta$ 40 in Alzheimer's disease is associated with a gene dosage effect of the apolipoprotein E E4 allele. *Neurosci Lett* 1997, 221:81-84
  43. Paresce DM, Ghosh RN, Maxfield FR: Microglial cells internalize aggregates of the Alzheimer's disease amyloid  $\beta$ -protein via a scavenger receptor. *Neuron* 1996, 17:553-565
  44. El Khoury J, Hickman SE, Thomas CA, Cao L, Silverstein SC, Loike JD: Scavenger receptor-mediated adhesion of microglia to  $\beta$ -amyloid fibrils. *Nature* 1996, 382:716-719
  45. Yan SD, Chen X, Fu J, Chen M, Zhu H, Roher A, Slattery T, Zhao L, Nagashima M, Morser J, et al.: RAGE and amyloid-beta peptide neurotoxicity in Alzheimer's disease. *Nature* 1996, 382:685-691
  46. Frautschy SA, Li A, Harris ME, Yang F, Cole GM: Factors promoting

- $A\beta$  deposition and toxicity in the rat. Soc Neurosci Abstr 1996, 22: 1910
47. Kiefer R, Streit WJ, Toyka KV, Kreutzberg GW, Hartung H: Transforming growth factor- $\beta$ 1: a lesion-associated cytokine of the nervous system. *Int J Dev Neurosci* 1995, 13(3/4):331-339
  48. Frautschy SA, Yang F, Calderón L, Cole GM: Rodent models of Alzheimer's disease: rat  $A\beta$  infusion approaches to amyloid deposits. *Neurobiol Aging* 1996, 17:311-321
  49. Rozemuller JM, Bots GTAM, Roos RAC, Eikelenboom P: Acute phase proteins but not activated microglial cells are present in parenchymal  $\beta$ /A4 deposits in the brains of patients with hereditary cerebral hemorrhage with amyloidosis-Dutch type. *Neurosci Lett* 1992, 140:137-140
  50. Gearing M, Wilson RW, Unger ER, Shelton ER, Chan HW, Masters CL, Beyreuther K, Mirra SS: Amyloid precursor protein (APP) in the striatum in Alzheimer's disease: an immunohistochemical study. *J Neuropathol Exp Neurol* 1993, 52:22-32
  51. Kida E, Golabek AA, Wisniewski T, Wisniewski KE: Regional differences in apolipoprotein E immunoreactivity in diffuse plaques in Alzheimer's disease brain. *Neurosci Lett* 1994, 167:73-76
  52. Uchihara T, Kondo H, Akiyama H, Ikeda K: White matter amyloid in Alzheimer's disease brain. *Acta Neuropathol* 1995, 90:51-56
  53. Kimura T, Hisano T, Yoshida H, Ueda K, Miyakawa T: Re-evaluation of classical senile plaques by three-dimensional analysis. *J Neurol* 1994, 241:624-627
  54. Selkoe DJ: Alzheimer's disease: a central role for amyloid. *J Neuropathol Exp Neurol* 1994, 53:438-447
  55. Lue LF, Brachova L, Civin WH, Rogers J: Inflammation,  $A\beta$  deposition, and neurofibrillary tangle formation as correlates of Alzheimer's disease neurodegeneration. *J Neuropathol Exp Neurol* 1996, 55: 1083-1088
  56. Mochizuki A, Peterson JW, Mufson EJ, Trapp BD: Amyloid load and neural elements in Alzheimer's disease and non-demented individuals with high amyloid plaque density. *Exp Neurol* 1996, 142:89-102